Synthesis of Spongelike Mesoporous Anatase and its Photocatalytic Properties

Janitabar Darzi, Simin
J. I. H. Research Laboratories, Nuclear Science and Technology Research Institute, P.O. Box 11365/8486 Tehran, I.R. IRAN

Mahjoub, Ali Reza*[+]
Department of Chemistry, Tarbiat Modares University, 14115-175 Tehran, I.R. IRAN

Nilchi, Abdolreza
J. I. H. Research Laboratories, Nuclear Science and Technology Research Institute, P.O. Box 11365/8486 Tehran, I.R. IRAN

ABSTRACT: *Mesoporous TiO_2 has been prepared using a nonionic block copolymer (Pluronic P-123) as structure-directing agent with sol-gel method. Characterization of the product was carried out by means of X-ray diffraction (XRD), scanning electron microscopy (SEM), thermogravimetry-differential scanning calorimetry (TG-DSC), Nitrogen sorption isotherms, and UV-vis absorption spectroscopy. These analyses showed that under controlled synthesis conditions, a wormlike mesostructured TiO_2 with high surface area (110 m^2g^{-1}) and appropriated band gap (~3 eV) is obtained. Moreover, the pore walls of the nanostructured TiO_2 solid are formed by incipient crystallites of anatase, which is a significant achievement regarding its possible photocatalytic applications. The activity of the prepared photocatalyst was evaluated by degradation of Congo Red azo dye. It has excellent photocatalytic efficiencies and more than 76% dye was decolorized in 90 minute.*

KEYWORDS: *Mesostructure, TiO_2, Anatase, Photochemical degradation.*

INTRODUCTION

TiO_2 is extensively studied for applications in sensors [1], solar energy conversion [2], catalysis [3], and optical coatings [4]. It is a semiconductor catalyst well-known for photodegradation of organic substances in water [5]. For many of these applications, the porosity, surface area, structure, crystal phase and particle size are factors that influence dramatically the activity and performance of titanium dioxide [6]. TiO_2 has three kinds of crystal phase: anatase, rutile and brookite. Anatase-type titania exhibits high photocatalytic activity and thus has recently attracted a great deal of attention in the field of photocatalysts for decomposition of environmental pollutants and antibacterial applications. Anatase nanocrystals exhibit high photocatalytic activity, compared to the bulk crystals, as they facilitate diffusion of excited electrons and holes toward the surface before their recombination. The spongy TiO_2 samples show good adsorption and high photocatalytic efficiency towards organic contaminants [7].

* *To whom correspondence should be addressed.*
+ E-mail: mahjouba@modares.ac.ir
1021-9986/09/2/35 5/$/2.50

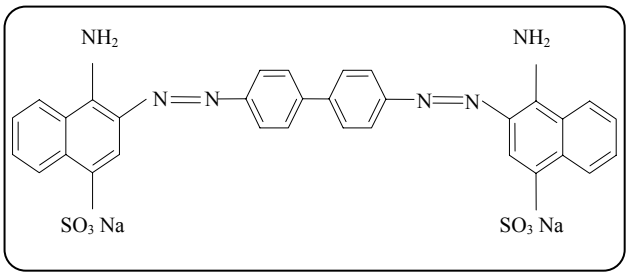

Fig. 1: Structure of Congo Red.

Producing porous TiO_2 samples with large surface area can improve its photocatalytic properties by means of reducing recombination rate of photo induced electron-hole pairs. This is due to their faster arrival to the reaction site of the surface.

In present work, synthesis of mesoporous anatase TiO_2 with a large surface area using the polymeric surfactant Pluronic P-123 and titanium tetrachloride as raw materials is described. The photocatalytic activity of the synthesized and commercial TiO_2 (Degussa P25) is investigated using artificial UV-C light for degradation of the azo-dye Congo Red (Fig. 1).

EXPERIMENTAL SECTION

Materials

The chemicals used in this study were titanium tetrachloride ($TiCl_4$), 99.9%, Fluka, as a titanium precursor, triblock copolymer Pluronic P-123 ($EO_{20}PO_{70}EO_{20}$), Aldrich, as template, Congo Red ($C_{32}H_{22}N_6Na_2O_6S_2$) and anhydrous ethanol (C_2H_5OH) from Merck. Commercial titanium dioxide, Degussa P25 (51 m^2g^{-1} nanoporous, 80% anatase and 20% rutile) was used as a reference photocatalyst was supplied by Degussa company.

Catalyst characterization

Powder phase identification and crystallite sizes of the product were performed by X-ray diffraction (XRD) obtained on Philips X-pert diffractometer using a scan rate of 2°/min and Cu Kα line (λ=1.54056Å) radiation with working voltage and current of 40 kV and 40 mA, respectively. The morphology and microstructure of the product were studied by scanning electron microscopy (SEM, Philips XL30). TG-DSC was carried out using STA 150 Rhenometric Scientific unit. Measurements were taken with a heating rate of 10 °C/min from 25 to 800 °C in argon atmosphere. Nitrogen sorption measurement of the sample was determined by (Quantachrome NOVA 2200 e). Spectroscopic analysis of TiO_2 was performed using UV-vis spectrophotometer (Shimadzu UV 2100).

Catalyst synthesis

The synthetic procedure was as follow:

Pluronic P-123 (0.9 g) was first dissolved in ethanol. The resulting solution was stirred for 1 h. Then 1 mL of titanium tetrachloride was added to the solution under vigorous stirring. The mixture was kept in a beaker at 40 °C for 5 days under constant stirring and more ethanol was added periodically. The solution was placed on a petri dish and dried in an oven at 40 °C for 48 h, and then calcined at 470 °C for 4 h. The calcined TiO_2 crystals were finally grinned.

Photocatalytic activity measurements

Photocatalytic activity of the synthesized TiO_2 and Degussa P25 were evaluated by the degradation of Congo Red. The experiments were conducted in glass cells (with 7.5 cm diameter) and in identical conditions. A 30 W UV-C lamp was used as light source. The distance between the UV source and the vessels containing reaction mixture was fixed at 15 cm. Air was continuously bubbled into the solution in order to provide a constant source of dissolved oxygen. 0.025 g of photocatalyst was placed in a 50 mL aqueous solution of 5 ppm Congo Red. Prior to irradiation, the suspension was magnetically stirred in the dark for approximately 10 min. Then the lamp was switched on to initiate the reaction. During irradiation, the suspension was sampled at regular intervals and immediately centrifuged to remove catalyst particles. The photocatalytic degradation was monitored by measuring the absorbance of the solution samples with UV-vis spectrophotometer.

RESULTS AND DISCUSSION

Characterization

Fig. 2 shows the wide-angel powder XRD patterns of synthesized TiO_2. The diffraction peaks can be indexed to the tetragonal structured anatase. The average crystallite size of the synthesized TiO_2 calculated to be 7.414 nm from *Scherer*'s equation [8].

Figs. 2 a and b show the low-angel XRD patterns of the synthesized and calcined TiO_2 samples, respectively. The partial ordered phase structurally collapsed and TiO_2

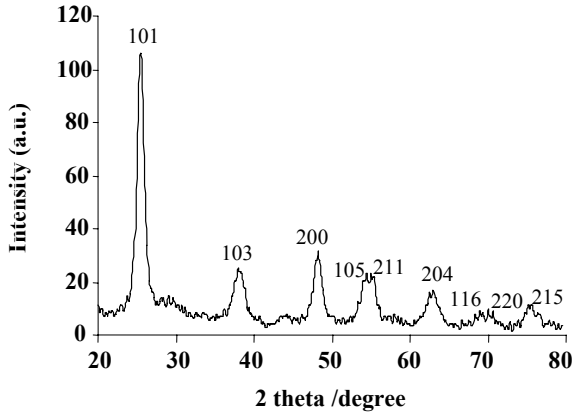

Fig. 2: Wide- angel XRD patterns of the calcined TiO_2 sample (with anatase lines shown for reference).

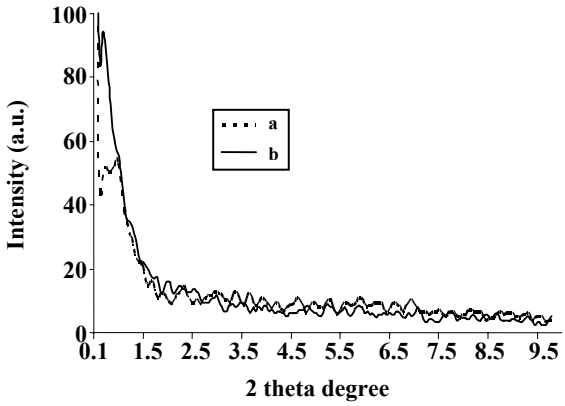

Fig. 3: Low-angel XRD pattern of synthesized (a) and calcined TiO_2 (b).

phases became disordered during the calcinations at 470 °C, as revealed by these XRD spectra. But according to Fig. 3 (b), there is a small peak in the 2Θ range of 0.5-1 corresponds to the wormlike mesostructure in the calcined TiO_2 sample [9]. It reveals that thickness of mesoporous titania walls is enough to bear the strong stress caused by phase transition in the calcination process [10].

Figs. 4 a and b show SEM images of synthesized TiO_2 after calcination. The images illustrate a general view of their morphology where the synthesized TiO_2 is spongy form and exhibits high porosity. In Fig. 4 a it could be seen that macropores with different sizes were formed. The macropores are distributed in the sample non-uniformly. The walls of the macropores composed of interconnected spherical TiO_2 particles are shown in the magnified SEM image (Fig. 4 b).

Differential thermal and thermogravimetric curves of the precipitate prior to calcination are shown in Fig. 5.

According to TG analysis, the weight loss consists of three distinct steps. The first stage (up to 100 °C) corresponds to removal of physically absorbed water. The second stage (up to 306 °C) is accompanied by significant exothermic peak in DSC curve which is attributed to the release of surfactant from the TiO_2. Finally, the weak thermal effect at 306-500°C is accompanied by obvious exothermic peak at around 470°C in DSC curve which confirms the crystallization of the amorphous phase to anatase. On the other hand, condensation reactions between the large amounts of uncondensed Ti–OH, existing on the surface of the amorphous mesoporous TiO_2, take place during calcination process and slow weight loss in the temperature range of 306-500 °C is mainly related to loss of water molecules due to condensation of Ti-OH groups [11]. However, direct observation of the exothermic effect in the DSC curve has been difficult, probably because the crystallization temperature is usually close to the decomposition temperatures of residual surfactant and removal of chemisorbed water, which are demonstrated as endothermic effects.

Fig. 6 shows the N_2-adsorption-desorption isotherms as a function of P/P_0. The macropores observed from the SEM images are too big to be reflected in the nitrogen adsorption isotherm. On the other hand, N_2 adsorption-desorption analyses could not provide macroporous information of the TiO_2 samples [12]. According to Fig. 6, isotherm is of type IV which proves the presence of mesopores within the synthesized sample [13]. The BET surface area is 110 m^2g^{-1} deduced from the plot. Desorption branch was used to obtain a pore size distribution of the prepared TiO_2 sample. The pore size distribution plot shows one peak that centers at 6.09 nm (shown in the inset of Fig. 6).

Fig. 7 shows optical absorption spectrum of mesoporous TiO_2 dispersed in ethanol, plotted as $(\alpha h\upsilon)^{1/2}$ versus photon energy ($h\upsilon$) where α represents optical absorption coefficient.

The optical band gap (E_g) in a semiconductor is determined by assuming the nature of transition (m) and plotting $(\alpha h\upsilon)^{1/m}$ versus ($h\upsilon$) where m represents the nature of transition. Now, m may have different values, such as 1/2, 2, 3/2 or 3 for allowed direct and indirect;

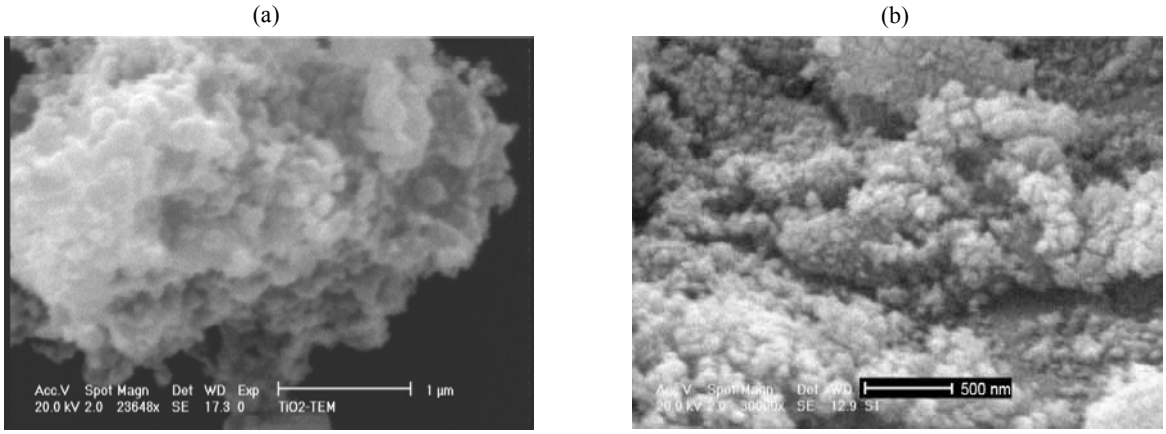

Fig. 4: SEM images of synthesized TiO_2 after calcination at scale 1µm (a) and 500 nm (b).

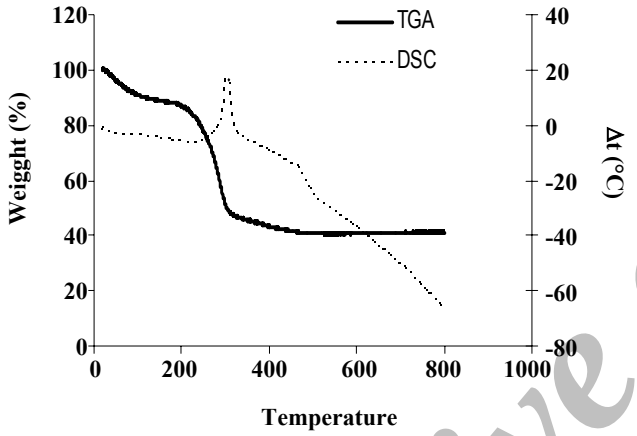

Fig. 5: TG-DSC curves for the TiO_2 before calcinations.

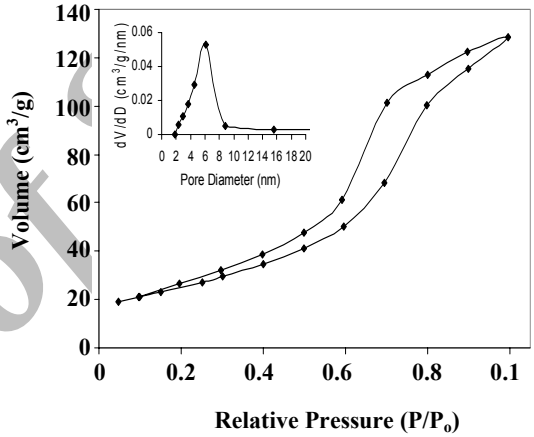

Fig. 6: N_2-adsorption-desorption isotherms, and inset: BJH pore size distribution curve of prepared mesoporous TiO_2.

and forbidden direct and indirect transitions, respectively [14]. For allowed indirect transition one can plot $(\alpha h\upsilon)^{1/2}$ versus hυ and extrapolate the linear portion of it to α = 0 value to obtain the corresponding band gap (E_g). The indirect band gap of this photocatalyst is obtained about 3 eV by this method. Synthesized mesoporous TiO_2 shows large red shift than commercial P25. The commercial P25 has an optical absorption edge of 380 nm (3.2 eV). Optical absorption at higher wavelength may be reduce the photocatalytic efficiency of the synthesized TiO_2 in comparison with the commercial ones.

Catalyst formation mechanism

Pluronic P-123 is commercially available symmetric triblock copolymers with Poly (Ethylene Oxide), PEO, as the hydrophilic end blocks and Poly (Propylene Oxide), PPO, as the hydrophobic middle block. The difference in hydrophobicity/hydrophilicity between the Poly (Ethylene Oxide) PEO and Poly (Propylene Oxide) PPO chains in low water content alcoholic media is not marked enough to give rise to Liquid Crystalline (LC) phases in the initial systems [15]. The interactions between the template and the inorganic component also depend on the solvent. The scarce water present in low water systems reacts promptly with the titania precursor, generating a set of hydrophobic clusters under these conditions [16]. These Ti–O clusters, can attach loosely to the hydrophobic PPO block; this process also tends to destabilize the formation of a well-ordered mesophase. On the other hand an ethoxide-modified titanium chloride, is formed by the reaction [17]:

$$TiCl_4 + x\ EtOH \rightarrow TiCl_{4-x}(OEt)_x + HCl$$

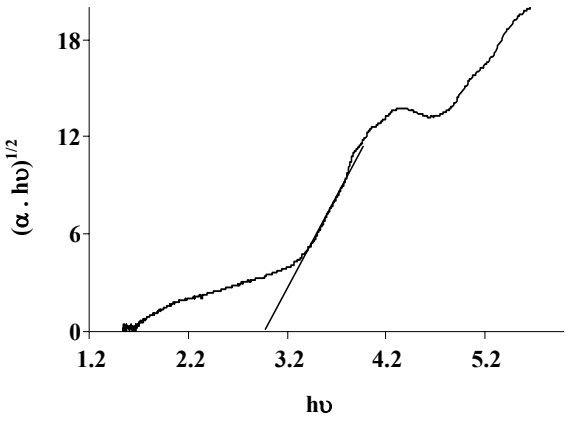

Fig. 7: Optical absorption spectrum of the dispersed mesoporous TiO_2 drawn as $(\alpha h\upsilon)^{1/2}$ versus photon energy (hυ).

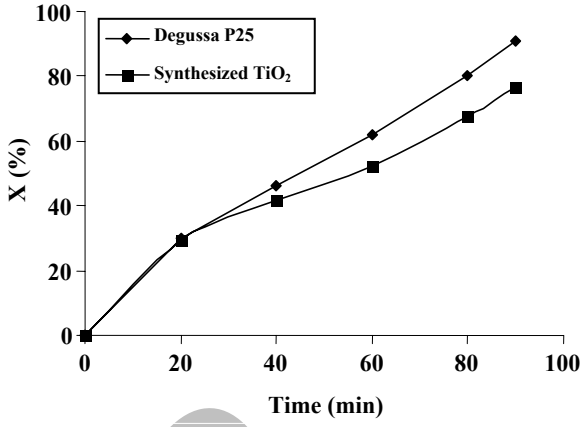

Fig. 8: The degree of photocatalytic degradation (X) as a function of irradiation time at 497 nm for synthesized TiO_2 and Degussa P25.

By heating the reaction mixture for 5 days at 40°C (see experimental section) the HCl evaporated. Transalcoholysis of the $–CH_2–CH_2–OH$ tips on the $TiCl_{4-x}(OEt)_x$ moieties ($0<x<2$) [18, 19], and chelation of titanium (IV) ions or oligomers by PEO or PPO blocks are two essential interactions between metal centers and the texturing agent. These interactions lead to unfolding of the polymer. The unfolding process disrupts the formation of an organized LC phase, based upon the self-assembly properties of the polymer. As a consequence, ill-defined channels develop all along the sample. Finally a spongelike titania mesopore is established after calcination and removing organic texturing agent.

Photocatalytic activity

Absorption peaks at 234, 347 and 497 nm are due to Congo Red. Photocatalytic degradation of Congo Red, results in smaller absorption bands. Fig. 8 shows the efficiency of photodegradation (X) as a function of time at 497 nm for synthesized nanostructured porous TiO_2 and commercial TiO_2. Here $X = (C_0-C)/C_0$, where C_0 is the initial concentration of dye, and C is the concentration of dye at time T. As shown in Fig. 8, synthesized TiO_2 photocatalyst has high efficiency in Congo Red decolorization but it is weaker than commercial P25. Two reasons for difference in reactivities of the catalysts are proposed. One of them could be that P25 has a well crystallized mixed crystalline structure (75% anatase and 25% rutile) that would be responsible for the photocatalysis superiority. Another reason that the study proposes is to be due to the larger red shift of our sample than commercial P25.

The prepared mesoporous TiO_2 disperses very well in water. However unlike Degussa P25, it does not form a turbid solution in water. Although the prepared TiO_2 catalyst is smaller in size compared to Degussa, it is however easy to separate from water by centrifugation for the above reason. Effective filtration is a good approach in photocatalytic studies.

CONCLUSIONS

This study demonstrates the possibility of preparation of sol–gel mesoporous TiO_2 photocatalyst using $TiCl_4$ and pluronic P-123 surfactant as raw materials. Calcination at 470 °C leads to loss of order and partial collapse of the mesostructure, but the synthesized TiO_2 maintains a significant level of porosity. Titania prepared by this method has a highly crystalline single anatase phase with complex structure of agglomerated nanoparticles. This structure gives a high degree of mesoporosity that corresponds to large surface area.

We show that titania prepared by this method exhibits good photocatalytic property but weaker than the commercial P25. We supposed that the well crystallized mixed crystalline structure of P25 would be responsible for the photocatalysis superiority in comparison with the synthesized mesoporous TiO_2, although the synthesized sample has larger surface area. The UV-Vis spectrum of

the synthesized TiO_2 showed a larger red shift than commercial P25. It would be another reason for lower photocatalytic activity of synthesized mesoporousTiO_2.

Acknowledgments

Support by Nuclear Science and Technology Research Institute of Atomic Energy Organization of Iran and Tarbiat Modares University is greatly appreciated.

Received : Oct. 27, 2008 ; Accepted : May 18, 2009

REFERENCES

[1] Jun Y., Kim H., Lee H.J., Hong S., CO Sensing Performance in Micro-Arc Oxidized TiO_2 Films for Air Quality Control, *Sensors and Actuators B.*, **120**, 69 (2006).

[2] Wang P., Zakeeruddin S., Exnar I., Grätzel M., High Efficiency Dye-Sensitized Nanocrystalline Solar Cells Based on Ionic Liquid Polymer Gel Electrolyte, *Chem. Commun.,* **1**, p. 2972 (2002).

[3] Kabra K., Chaudhary R., Sawhney R., Treatment of Hazardous Organic and Inorganic Compounds Through Aqueous-Phase Photocatalysis: A Review, *Ind. Eng. Chem. Res.,* **43**, p. 7683 (2004).

[4] Roy D., Fendler J., Reflection and Absorption Techniques for Optical Characterization of Chemically Assembled nanomaterials, *Adv. Mater.*, **16**, p. 479 (2004).

[5] Mahmoodi N.M., Arami M., Yousefi Limaee N., Salman Tabrizi N., Kinetics of Heterogeneous Photocatalytic Degradation of Reactive Dyes in an Immobilized TiO_2 Photocatalytic, *J. Colloid Interf. Sci.,* **295**, p. 159 (2006).

[6] Alvaro M., Aprillle C., Benitez M., Carbonell E., Garcia H., Photocatalytic Activity of Structured Mesoporous TiO_2 Materials, *J. Phys. Chem. B.*, **110**, p. 6661 (2006).

[7] Jia X., He W., Yang W., Zhao H., Zhang X., Nanomorphological Anatase TiO_2: From Spongy Network to Porous Nanoparticles, *Mat. Let.*, **62**, p. 1896 (2008).

[8] Patterson A.L., The Scherrer Formula for X-Ray Particle Size Determination, *Phys Rev.*, **56**, p. 978 (1993).

[9] Li X.S., Fryxell G.E., birnbaum J.C., Wang C., Effects of Template and Precursor Chemistry on Structure and Properties of Mesoporous TiO_2 Thin Films, *Langmuir,* **20**, p. 9095 (2004).

[10] Grosso D., Soler-Illia G.J.A.A., Crepaldi E.L., Cegnol C., Sinturel A., Bourgeois A., Brunet-Bruneau A., Amenitsch H., Albouy P.A., Sanchez C., Highly Porous TiO_2 Anatase Optical Thin Films with Cubic Mesostructure Stabilized at 700 °C, *Chem. Mater.,* **15**, p. 4562 (2003).

[11] Xiao J., Peng T., Li R., Peng Z., Yan C., Preparation Phase Transformation and Phtocatalytic Activities of Cerium-Doped Mesoporous Titania Nanoparticles, *J. Solid State Chem.*, **179**, p. 1161 (2006).

[12] Yu J., Zhang L., Cheng B., Su Y., Hydrothermal Preparation and Photocatalytic Activity of Hierarchically Sponge-Like Marco-/Mesoporous Titania, *J. Phys. Chem. C* **111**, p. 10582 (2007).

[13] Wark N., Tschirch J., Bartels O., Bahnemann D., Rathousky J.,Photocatalytic Activity of Hydrophobized Mesoporous Thin Films of TiO_2, *Micropor. Mesopor. Mater.,* **84**, p. 247 (2005).

[14] Bhattacharyya D., Chaudhuri S., Pal A.K., Bandgap and Optical Transitions in thin Films from Reflectance Measurements, *Vacuum,* **43**, p. 313 (1992).

[15] Alexandridis P., Zhou D., Khan A., Lyotropic Liquid Crystallinity in Amphiphilic Block Copolymers: Temperature Effects on Phase Behavior and Structure for Poly(Ethylene Oxide)-b-Poly(Propylene Oxide)-b-Poly(Ethylene Oxide) Copolymers of Different Composition, *Langmuir*, **12**, p. 2690 (1996).

[16] Blanchard J., Ribot F., Sanchez C., Bellot P.V., Trokiner A., Structural Characterization of Titanium-Oxo-Polymers Synthesized in the Presence of Protons or Complexing Ligands as Inhibitors, *J. Non-cryst. Solids,* **265**, p. 83 (2000).

[17] Brinker C.J., Scherer G.W., Sol-Gel Science: The Physics and Chemistry of Sol-Gel Processing, "Sol-Gel Science", p.54, Academic Press, San Diego, (1990).

[18] Yang P., Zhao D., Margolese D.I., Chmelka B.F., Stucky G.D.,Block Copolymer Templating Syntheses of Mesoporous Metal Oxides with Large Ordering Lengths and Semicrystalline Framework, *Chem. Mater.*, **11**, p. 2813 (1999).

[19] Yang P., Zhao D., Margolese D.I., Chmelka B.F., Stucky G.D., Generalized Syntheses of Large-Pore Mesoporous Metal Oxides with Semicrystalline Frameworks, *Nature*, **396**, p. 152 (1998).